12-12-2017

No Consistent Evidence for Advancing or Delaying Trends in Spring Phenology on the Tibetan Plateau

Xufeng Wang
Chinese Academy of Sciences

Jingfeng Xiao
University of New Hampshire, Durham, j.xiao@unh.edu

Xin Li
Chinese Academy of Sciences

Guodong Cheng
Chinese Academy of Sciences

Mingguo Ma
Southwest University

See next page for additional authors

Recommended Citation
Wang, X.*, Xiao, J., Li, X., Cheng, G., Ma, M., Che, T., Dai, L., Wang, S., Wu, J. (2017) No consistent evidence for advancing or delaying trends in spring phenology on the Tibetan Plateau. Journal of Geophysical Research: Biogeosciences, 122, 3288–3305, DOI: 10.1002/2017JG003949.

AGU PUBLICATIONS

JGR

Journal of Geophysical Research: Biogeosciences

RESEARCH ARTICLE
10.1002/2017JG003949

Key Points:
- The trend in spring phenology on the Tibetan Plateau varied among the five NDVI data sets and between the two phenology retrieval methods
- There was no consistent evidence for advancing or delaying trends in spring phenology on the Tibetan Plateau
- The debate on the trends of spring phenology could be largely attributed to the use of different NDVI data sets and/or different methods

Supporting Information:
- Supporting Information S1
- Figure S1
- Figure S2
- Figure S3
- Figure S4
- Figure S5
- Figure S6
- Figure S7
- Figure S8

Correspondence to:
X. Wang and J. Xiao,
wangxufeng@lzb.ac.cn;
j.xiao@unh.edu

Citation:
Wang, X., Xiao, J., Li, X., Cheng, G., Ma, M., Che, T., … Wu, J. (2017). No consistent evidence for advancing or delaying trends in spring phenology on the Tibetan Plateau. *Journal of Geophysical Research: Biogeosciences*, *122*, 3288–3305. https://doi.org/10.1002/2017JG003949

Received 18 MAY 2017
Accepted 5 DEC 2017
Accepted article online 12 DEC 2017
Published online 23 DEC 2017

No Consistent Evidence for Advancing or Delaying Trends in Spring Phenology on the Tibetan Plateau

Xufeng Wang[1,2], Jingfeng Xiao[2], Xin Li[1,3], Guodong Cheng[1], Mingguo Ma[4], Tao Che[1], Liyun Dai[1], Shaoying Wang[5], and Jinkui Wu[6]

[1]Key Laboratory of Remote Sensing of Gansu Province, Heihe Remote Sensing Experimental Research Station, Cold and Arid Regions Environmental and Engineering Research Institute, Chinese Academy of Sciences, Lanzhou, China, [2]Earth Systems Research Center, Institute for the Study of Earth, Oceans, and Space, University of New Hampshire, Durham, NH, USA, [3]CAS Center for Excellence in Tibetan Plateau Earth Sciences, Chinese Academy of Sciences, Beijing, China, [4]School of Geographical Sciences, Southwest University, Chongqing, China, [5]Key Laboratory of Land Surface and Climate Change in Cold and Arid Regions, Cold and Arid Regions Environmental and Engineering Research Institute, Chinese Academy of Sciences, Lanzhou, China, [6]State Key Laboratory of Cryospheric Sciences, Cold and Arid Regions Environmental and Engineering Research Institute, Chinese Academy of Sciences, Lanzhou, China

Abstract Vegetation phenology is a sensitive indicator of climate change and has significant effects on the exchange of carbon, water, and energy between the terrestrial biosphere and the atmosphere. The Tibetan Plateau, the Earth's "third pole," is a unique region for studying the long-term trends in vegetation phenology in response to climate change because of the sensitivity of its alpine ecosystems to climate and its low-level human disturbance. There has been a debate whether the trends in spring phenology over the Tibetan Plateau have been continuously advancing over the last two to three decades. In this study, we examine the trends in the start of growing season (SOS) for alpine meadow and steppe using the Global Inventory Modeling and Mapping Studies (GIMMS)3g normalized difference vegetation index (NDVI) data set (1982–2014), the GIMMS NDVI data set (1982–2006), the Moderate Resolution Imaging Spectroradiometer (MODIS) NDVI data set (2001–2014), the Satellite Pour l'Observation de la Terre Vegetation (SPOT-VEG) NDVI data set (1999–2013), and the Sea-viewing Wide Field-of-View Sensor (SeaWiFS) NDVI data set (1998–2007). Both logistic and polynomial fitting methods are used to retrieve the SOS dates from the NDVI data sets. Our results show that the trends in spring phenology over the Tibetan Plateau depend on both the NDVI data set used and the method for retrieving the SOS date. There are large discrepancies in the SOS trends among the different NDVI data sets and between the two different retrieval methods. There is no consistent evidence that spring phenology ("green-up" dates) has been advancing or delaying over the Tibetan Plateau during the last two to three decades. Ground-based budburst data also indicate no consistent trends in spring phenology. The responses of SOS to environmental factors (air temperature, precipitation, soil temperature, and snow depth) also vary among NDVI data sets and phenology retrieval methods. The increases in winter and spring temperature had offsetting effects on spring phenology.

1. Introduction

Vegetation phenology is the timing of seasonal growth stages in vegetation life cycles, such as budburst, leaf unfolding, flowering, and senescence. Plant phenology is controlled by a suite of climatic and biotic factors, and the changes of phenology have significant effects on the exchange of carbon, water, and energy between ecosystems and the atmosphere (Penuelas et al., 2009). Vegetation phenology has received growing attention in global change research because of its sensitivity to climate change and effects on carbon, water, and energy cycling (Badeck et al., 2004; Richardson et al., 2013). In the recent two decades, the satellite-derived normalized difference vegetation index (NDVI) has been widely used to estimate the timing of start of growing season (SOS) at regional scales (Zhang et al., 2003). It has been reported that spring phenology has been advancing in some parts of the Northern Hemisphere because of climatic warming (Menzel et al., 2006), while this trend is decreasing as a result of warming-related reduction in chilling (Fu et al., 2015).

The Tibetan Plateau, the Earth's "third pole" has witnessed rapid warming during the last several decades (Duan & Xiao, 2015; Zhong et al., 2011). The Tibetan Plateau is a unique region for studying the responses of vegetation phenology to climate change and their feedbacks to the climate because of the high sensitivity of alpine vegetation to climate and the low-level human disturbance. Quantifying the trends in spring

phenology on the Tibetan Plateau is important for understanding the carbon, water, and energy cycling of the plateau and the interactions between the alpine ecosystems and the regional climate. The trends in spring phenology over the Tibetan Plateau have been highly controversial. By using the Moderate Resolution Imaging Spectroradiometer (MODIS), Satellite Pour l'Observation de la Terre (SPOT) Vegetation (SPOT-VEG), and Global Inventory Modeling and Mapping Studies (GIMMS) NDVI data sets and the polynomial fitting and NDVI threshold method, Zhang et al. (2013) argued that the SOS of the Tibetan Plateau had been continuously advancing with a rate of 1.04 d/yr from 1982 to 2011 and an even greater rate during the period from 2000 to 2011 than the period from 1982 to 2000. Yu et al. (2010) reported that the SOS of the Tibetan Plateau derived from the GIMMS NDVI data set using the polynomial fitting and NDVI threshold method advanced from 1982 to the mid-1990s and retreated after the mid-1990s because of the increasing winter temperature and spring temperature. By contrast, some other studies reported that no significant SOS trend was found from 1982 to 2013 (Ding et al., 2016; Liu et al., 2016). Ding et al. (2016) used the polynomial method and the GIMMS3g (version 0) and SPOT-VEG data, while Liu et al. (2016) used the logistic method (logistic fitting and NDVI inflection detecting) and the advanced very high resolution radiometer (AVHRR) and MODIS data. T. Wang et al. (2013) found that the continuously advancing trend in SOS derived from MODIS and SPOT-VEG NDVI was significantly correlated with the increasing NDVI in January–April induced by the deceasing snow cover fraction. Shen et al. (2013) removed the NDVI increasing effect during the nongrowing season and found no trend in the SOS retrieved from the SPOT-VEG NDVI data set using the same method as used by Zhang et al. (2013). The use of different NDVI data sets and/or phenology retrieval methods could lead to the discrepancies in the SOS trends among these studies. Field phenological observations showed that only one of 11 plant species exhibited a significant advancing trend in SOS from 1990 to 2006, and no species had a delaying SOS trend (Zhou et al., 2014). Settling the debate on the trends in spring phenology on the Tibetan Plateau will improve our understanding of the responses of alpine ecosystems to climate change and their feedbacks to the climate.

The spring phenology of the Tibetan Plateau is controlled by a variety of environmental factors (e.g., air temperature, precipitation, soil temperature, and snow cover). The mechanisms of the trends in the SOS of the Tibetan Plateau have also been debated. Yu et al. (2010) reported that increasing spring temperature resulted in the advance of SOS, while increasing winter temperature led to the delay of SOS because of failure of chilling. Zhang et al. (2013) showed that both spring and winter temperature was negatively correlated with SOS, indicating that increasing winter temperature also led to the advance of SOS. A recent study based on field phenology observations did not find evidence for delaying SOS induced by warming winter (Chen et al., 2015). Precipitation at near half of the meteorological stations on the Tibetan Plateau was significantly correlated with SOS (Shen et al., 2011). The discrepancies on the relationships between SOS and environmental factors could be partly attributed to the scarcity of meteorological data and the quality of remote sensing data. The relative contributions of the environmental factors (e.g., air temperature, precipitation, and snow cover) on spring phenology on the Tibetan Plateau still remain unclear.

In this study, we assessed the consistency of the trends in SOS on the Tibetan Plateau using different satellite-derived NDVI records and SOS retrieval methods. We used the five long-term NDVI records that are currently available: the GIMMS NDVI data set (1982–2006), the GIMMS 3g NDVI data set (GIMMS3g, 1982–2015), the SPOT-VEG NDVI data set (1999–2013), the MODIS NDVI data set (MODIS, 2001–2014), and the Sea-viewing Wide Field-of-View Sensor (SeaWiFS) land NDVI data set (SeaWiFS, 1998–2007). For each NDVI record, two widely used SOS retrieval methods were used in this study. We also examined the effects of environmental factors (air temperature, precipitation, soil temperature, and snow cover) on SOS. The specific objectives of this study are to (1) assess the consistency of the trends in SOS on the Tibetan Plateau using different satellite-derived NDVI records and SOS retrieval methods, (2) evaluate the accuracy and trends of SOS derived from different data sets and methods on the Tibetan Plateau using eddy covariance gross primary productivity (GPP) and field phenological data, and (3) examine the relationships between satellite-derived SOS and a variety of environmental factors.

2. Data and Methods

2.1. Study Region

Our study region is the Tibetan Plateau (aka the Qinghai-Tibetan Plateau). The Tibetan Plateau covers ~2.4×10^6 km of land area, accounting for approximately one fourth of China's land territory. It is the

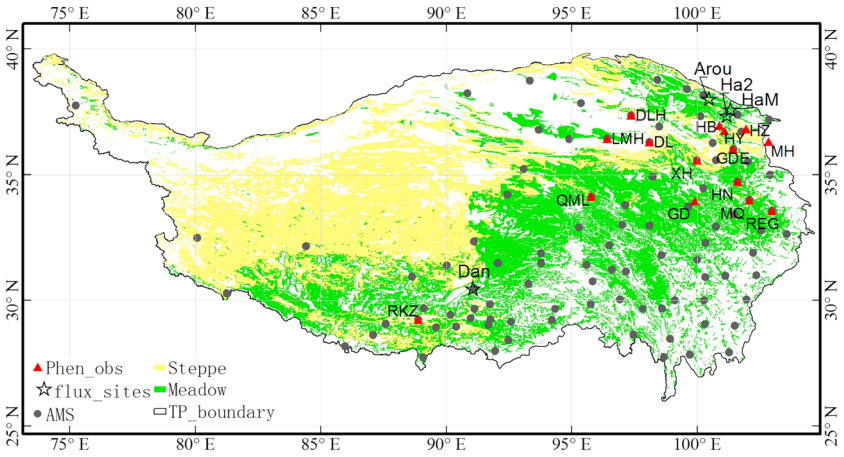

Figure 1. Distribution of the alpine meadow and steppe on the Tibetan Plateau and the location of phenology observing sites, eddy covariance flux towers, and meteorological stations (AMS).

highest plateau in the world with the average elevation over 4,500 m. The terrestrial ecosystems on the plateau are dominated by alpine meadow/steppe (Figure 1). Alpine meadow and steppe cover over 56% of the entire plateau area (Hou, 2001). Based on meteorological observations from weather stations, the multiyear mean annual precipitation and temperature of the plateau are 480 mm and 3.7°C, respectively.

The alpine meadow and steppe over the Tibetan Plateau are sensitive to climate change (Ganjurjav et al., 2015; Zhou et al., 2006). In this study, SOS of the Tibetan Plateau was estimated for alpine meadow and alpine steppe with remotely sensed NDVI data sets and then evaluated with in situ observations. We also examined the SOS trend and its relationship with meteorological factors. The grassland distribution and observation sites are shown in Figure 1.

2.2. Remote Sensing NDVI Data Sets

2.2.1. MODIS NDVI

The Moderate Resolution Imaging Spectroradiometer (MODIS) NDVI product (MOD13A2) is available at 16 day intervals and 1 km spatial resolution (Huete et al., 2002; Justice et al., 1998). This product is generated from atmospherically corrected bidirectional surface reflectance that had been masked for water, clouds, heavy aerosols, and cloud shadows. The Collection 6 of MOD13A2 from 2001 to 2014 for the Tibetan Plateau was obtained in this study. Precomposited surface reflectance data were used in Collection 6 vegetation index algorithm (Didan et al., 2015).

2.2.2. SPOT Vegetation NDVI

The Satellite Pour l'Observation de la Terre Vegetation (SPOT-VEG) NDVI product is available from 1999 to 2013 with a 1 km spatial resolution. SPOT-VEG was produced by merging 10 day segments using the maximum value composite method (Deronde et al., 2014). This data set is processed and distributed by the Flemish Institute for Technological Research (VITO) in Belgium. The data set was processed by atmospheric correction, radiometric correction, and geometric correction.

2.2.3. SeaWiFS NDVI

The Sea-viewing Wide Field-of-view Sensor (SeaWiFS) land NDVI data (McClain et al., 2004) are available at 15 day intervals and 4 km spatial resolution. The SeaWiFS NDVI data from 1998 to 2007 were obtained for the Tibetan Plateau. This data set is processed and distributed by the Ocean Biology Processing Group. After mid-2008, the SeaWiFS sensor experienced malfunctions that lasted until the end of the mission. Therefore, the SeaWiFS NDVI data since 2008 were not used in this study.

2.2.4. GIMMS and GIMMS3g NDVI

The GIMMS NDVI data were derived from the advanced very high resolution radiometer (AVHRR) instruments on board the National Oceanic and Atmospheric Administration's polar-orbiting meteorological satellites. The GIMMS NDVI data set that extends from 1981 (July) to 2006 (Tucker et al., 2005) has been widely used in ecological studies. The GIMMS NDVI data set is available at half-monthly interval and 8 km spatial resolution. Various corrections such as cloud contamination, sensor calibration, view geometry, and volcanic aerosols were performed to this data set before its release (Holben, 1986).

The GIMMS NDVI3g (GIMMS3g) NDVI data set is the latest version of the GIMMS NDVI data set and has been recently extended to the year of 2015 (Pinzon & Tucker, 2014). This data set was processed for minimizing various deleterious effects including calibration loss, orbital drift, intersensor inconsistency, and volcanic eruptions. It has the same spatial and temporal resolution as GIMMS. In this study, we used both GIMMS and GIMMS3g.

2.3. Snow Depth Data

A long-term snow depth product in China derived from passive microwave remote sensing data was used in this study to assess the snow effects on SOS. This snow depth product was generated by accounting for the intersensor calibration and was evaluated using field snow measurements and other independent data sets (Dai et al., 2015). The spatial and temporal resolutions of this data set are 0.25° and 1 day, respectively. The winter and spring snow depth was calculated as the average daily snow depth from November of the previous year to March and from April to May, respectively.

2.4. Meteorological Data

The monthly temperature and precipitation data from 1982 to 2014 were obtained from 95 meteorological stations across the Tibetan Plateau (Figure 1). These data sets were provided by the Climatic Data Center, National Meteorological Information Center, China Meteorological Administration. A total of 74 stations is located in meadow and steppe areas. Winter and spring temperatures for the vegetated regions were calculated as the average monthly temperature from November of the previous year to March and from April to May, respectively. Winter and spring precipitation for the vegetated regions was calculated as the cumulative precipitation from November of the previous year to March and from April to May, respectively.

2.5. Carbon Flux Data and Field Phenology Observations

Gross primary productivity (GPP) data from six eddy covariance flux sites (Figure 1) on the Tibetan plateau were used to evaluate the SOS derived from remote sensing data. Because the seasonal carbon uptake curves show the seasonal cycles of the ecosystems, carbon flux data can be used to evaluate the SOS derived from remote sensed NDVI (Balzarolo et al., 2016). Carbon flux of the Arou (Li et al., 2009; Li et al., 2013), Maqu (Wang et al., 2016), and Suli sites (Wu et al., 2015) were processed using the gap filling and partitioning tool in the statistics package-R provided by FLUXNET (https://www.bgc-jena.mpg.de/bgi/index.php/Services/REddyProcWebRPackage/) (Lasslop et al., 2010), and carbon flux data of other three sites were provided by FLUXNET (http://fluxnet.fluxdata.org/data/fluxnet2015-dataset/). The HaM (Zhao et al., 2006), Dan (Shi et al., 2006), Suli, Maqu, and Arou sites are grasslands, and Ha2 (Zhao et al., 2005) is a shrubland site. The daily GPP was smoothed by averaging with a 15 day moving window. The date when daily GPP exceeds 1 $gC/m^2/d$ during spring was determined as the field-based land surface SOS (Richardson et al., 2010).

Field phenology observations (Guo et al., 2011; Xu et al., 2014) were used to evaluate the SOS trend. This data set consists of observed budburst and senescence dates and starts from 1992. For grassland sites, a 50 m × 50 m plot in homogeneous area was selected as permanent plot to observe phenology date, and grazing is forbidden during grass growth and development period. Observers were trained according to the measuring criterion. The onset of the growing season was determined as the date when 50% grass in the sample plot became green by the observer's eyes (China Meteorological Administration, 1993). The observers were trained by the China Meteorological Administration (CMA). Field phenology observation sites are shown in Figure 1.

2.6. Data Analysis

2.6.1. Processing of NDVI Data

To further reduce the noise in NDVI, the Savizky-Golay filter was performed to all the NDVI data sets. NDVI usually changes slowly with the development of vegetation canopy, and an abrupt change point in the NDVI time series is considered as noise. The Savizky-Golay filter can remove this noise by smoothing the NDVI time series curve. The formula and parameters of the Savizky-Golay filter for alpine vegetation have been described in a previous paper (X. F. Wang et al., 2013). To minimize the effects of soil background on NDVI in sparsely vegetated areas, the pixels with multiyear mean NDVI < 0.1 were masked out. The growing season average NDVI (NDVI_gs) was calculated as the average NDVI from April to October for each data set. The annual average NDVI (NDVI_year) was calculated as the average NDVI from January to December for each data set. The seasonal average NDVI for winter (NDVI_wit), spring (NDVI_spr), summer (NDVI_smr), and

autumn (NDVI_aut) was calculated as the average NDVI from November of previous year to March, from April to May, from June to August, and from September to October, respectively. The NDVI for different vegetation types was calculated based on the Vegetation Type Map of China (Zhang et al., 2007).

2.6.2. SOS Retrieval, Trend Analysis, and Evaluation

SOS can be derived from the inflections in the curvature of the NDVI time series. Vegetation phenology can be represented using a series of double logistic functions which are built by fitting satellite-derived NDVI data to time (Julien & Sobrino, 2009; Zhang et al., 2003). The temporal variation in NDVI for a single growth or senescence cycle can be modeled using a logistic function as follows:

$$y(t) = a + b\left(\frac{1}{1+e^{c(t-d)}} + \frac{1}{1+e^{e(t-f)}}\right) \tag{1}$$

where t is time in days; $y(t)$ is the NDVI value at time t; c, d, e, and b are fitting parameters; $a + b$ is the maximum NDVI value, and a is the initial background NDVI value. The inflections in the change rate curve of the smoothed NDVI are used to determine the phenological dates. Specifically, the transition dates correspond to the times at which the second-order derivative of the smoothed NDVI time series exhibits local minima or maxima. During the growth period, these dates corresponding to the two local maxima points are the start of growing season (SOS) and the onset of maturity.

Another method of SOS estimation is to detect the NDVI change to a threshold NDVI value which is determined from the rate of seasonal changes in the multiyear mean NDVI seasonal curves. Specifically, the first step is to calculate the multiyear mean NDVI seasonal curve. The second step is to determine the change rate ($NDVI_{ratio}$) of multiyear mean NDVI seasonal curve using the following equation:

$$NDVI_{ratio} = \frac{NDVI(t+1) - NDVI(t)}{NDVI(t)} \tag{2}$$

where NDVI(t + 1) and NDVI(t) are NDVI value at time t + 1 and t, respectively; the third step is to obtain the NDVI value in multiyear average NDVI seasonal curve corresponding to the time of maximum change rate ($NDVI_{ratio}$) as the threshold SOS NDVI value. The fourth step is to fit the NDVI from January to September in each year to Julian Day using a polynomial function as follows:

$$NDVI = a + a1\times t + a2\times t^2 + \ldots + an\times t^n \qquad n = 6 \tag{3}$$

where t is Julian day in a year and a, $a1$ … $a6$ are fitting parameters. The final step is to determine the SOS date, when fitted NDVI is greater than threshold NDVI value (Reed et al., 1994; Zhang et al., 2013).

We used both methods to retrieve SOS for each year for each long-term NDVI data set on a per pixel basis. Flux tower GPP data were used to evaluate the SOS retrieved from the NDVI data sets for the pixels in which the eddy covariance flux towers are located. Daily GPP was smoothed by averaging with a 15 day moving window. The day when smoothed daily GPP exceeds 1 $gC/m^2/d$ was determined as tower SOS for evaluating the SOS derived from NDVI data sets. We then examined the trends of spatially avearged SOS for alpine meadow, alpine steppe, and the entire plateau using the five data sets and the two retrieval methods. The trends in SOS were also compared among different data sets and between the two retreival methods for the overlapping period of the five NDVI data sets (2001–2006); the entire period of each NDVI data set; the overlapping period of MODIS, SPOT-VEG, and GIMMS3g (2001–2013); and the overlapping period of GIMMS, GIMMS3g, and SeaWiFS (1998–2006), respectively. We also examined the trends in the SOS based on in situ phenology observations. For each site, the in situ phenology observations were also used to examine the trends in SOS at the site level; the observations were also used to evaluate the trends in SOS derived from the long-term NDVI data sets for the pixel in which the site is located.

The linear trends in SOS were calculated using the Mann-Kendall method. The Mann-Kendall method is a nonparametric test for monotonic trends. This method does not assume a specific distribution for the data and is not sensitive to outliers. When a monotonic trend is determined by the Mann-Kendall test, the Theil-Sen method can be used to calculate the slope of the trend (Sen, 1968). The slope of the trend measures the SOS change rate with time.

2.6.3. Environmental Controls of SOS Trends

We examined the controls of environmental factors (air temperature, soil temperature at 0 cm, precipitation, and snow depth) on spring phenology using correlation analysis. We first analyzed the relationship between

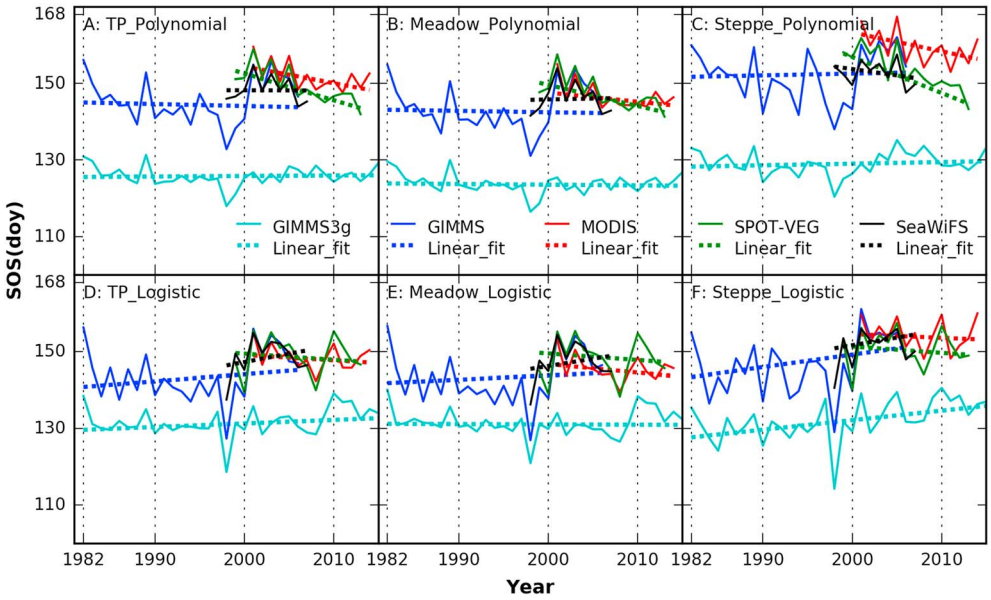

Figure 2. Start of growing season (SOS) of the Tibetan Plateau retrieved from the GIMMS3g, GIMMS, MODIS, SPOT-VEG, and SeaWiFS NDVI data sets. Dotted lines are the linear fitting lines based on the Theil-Sen method at confidence degree 0.95. The trend slopes and *P* values are provided in Table S1. TP: the entire Tibetan Plateau including both alpine meadow and steppe areas, Meadow: alpine meadow areas, Steppe: alpine steppe areas, Polynomial: threshold SOS method using polynomial function fitting, Logistic: inflection point SOS method using double logistic function fitting.

SOS and each environmental factor using correlation. We also used partial correlation analysis to examine the relative effects of these factors on SOS. Partial correlation measures the strength and direction of the relationship between two variables while controlling for the effects of one or more other variables. The trend analysis was also applied to environmental factors (e.g., air temperature, precipitation, soil temperature, and snow depth) to determine whether these factors exhibited significant trends.

3. Results

3.1. Long-Term Trends in Spring Phenology on the Tibetan Plateau

We first examined the trends of spatially averaged SOS for alpine meadow, alpine steppe, and the entire Tibetan Plateau using the GIMMS3g, GIMMS, MODIS, SPOT-VEG, and SeaWiFS NDVI data sets and both polynomial and logistic retrieval methods (Figure 2). For both methods, the SOS based on GIMMS3g was systematically lower than that based on other data sets. The SOS retrieved from MODIS, SPOT-VEG, and SeaWiFS was similar to one another in magnitude for alpine meadow, particularly for the polynomial method. For alpine steppe, the SOS exhibited larger differences in magnitude particularly for the polynomial method. The SOS of GIMMS was much larger than that of GIMMS3g and was close to that of MODIS, SPOT-VEG, and SeaWiFS after 2000. GIMMS-based SOS significantly advanced from 1982 to 1998 and significantly delayed after 1998, which was generally consistent with the results of two previous studies. The trends in SOS were greatly different between the two retrieval methods. Both MODIS SOS and SPOT-VEG SOS based on the polynomial method showed statistically significant advancing trends for both the entire Tibetan Plateau and the alpine meadow area (Table 1). For the logistic method, however, no significant advancing trend in SOS was found for any NDVI data set; only GIMMS3g SOS for alpine steppe exhibited a significant delaying trend. The consistency in the trends of SOS among different data sets was higher in the meadow area than in the steppe area.

3.2. Spatial Patterns of SOS Trends

To compare the spatial patterns of SOS retrieved from different data sets and different methods, we examined the mean SOS during the same period (from 2001 to 2006) for all five data sets and both methods (Figure 3). Generally, the mean SOS showed similar spatial patterns among different data sets except

Table 1
Theil-Sen Slope and P Value for SOS on the Tibetan Plateau Retrieved From Different NDVI Data Sets and Different Methods

	Theil-Sen slope					*P* value				
	GIMMS3g	GIMMS	MODIS	SPOT-VEG	SeaWiFS	GIMMS3g	GIMMS	MODIS	SPOT-VEG	SeaWiFS
TP_polynomial	0.013	−0.051	−0.431	−0.692	−0.008	0.70	0.82	0.05	< 0.01	0.71
Meadow_polynomial	−0.018	−0.036	−0.240	−0.551	0.047	0.27	0.87	0.04	< 0.01	0.86
Steppe_polynomial	0.042	0.046	−0.493	−0.933	−0.328	0.48	0.73	0.10	< 0.01	0.44
TP_logistic	0.092	0.182	−0.141	−0.159	0.079	0.16	0.43	0.31	0.99	0.45
Meadow_logistic	−0.008	0.130	−0.220	−0.170	−0.106	0.90	0.58	0.22	0.97	0.53
Steppe_logistic	0.249	0.324	−0.098	−0.165	0.402	< 0.01	0.13	0.63	0.89	0.34

GIMMS3g and between the two methods, and the eastern plateau had earlier SOS than the western counterpart. The GIMMS3g SOS was much earlier than that of other data sets. The mean SOS based on the logistic method generally followed unimodal distributions, while the mean SOS based on the polynomial method generally followed multimodal distributions (Figure S1 in the supporting information). For each retrieval method, the distribution of the mean SOS was similar among different data sets except for GIMMS3g.

To compare the differences in the SOS trends among the five NDVI data sets and between the two methods, we estimated the SOS trend during the entire period of each NDVI data set and the overlapping periods of these data sets (from 2001 to 2013 for MODIS, SPOT-VEG, and GIMMS3g and from 1998 to 2006 for GIMMS and SeaWiFS) (Figure 4). The trends exhibited large discrepancies between the two methods and among the different NDVI data sets for the same period. The pixels with a significant advancing trend in SOS accounted for a larger land area for the polynomial method than for the logistic method for all the data sets (Figures 4 and S2 and Table S1). For the polynomial method, the percentage of the pixels with significant advancing trends in SOS ranged from 5.4% (GIMMS3g: 2001 to 2013) to 34.7% (SPOT-VEG: 2001 to 2013), and the percentage of pixels with significant delaying trends in SOS ranged from 0.07% (SPOT-VEG: 2001 to 2013) to 4.1% (GIMMS3g: 2001 to 2013). For the polynomial method, the percentage of the pixels with significant advancing trends in SOS ranged from 1.1% (GIMMS3g: 2001 to 2013) to 6.6% (SPOT-VEG: 2001 to 2013). Among the five data sets, SPOT-VEG showed the largest area with advancing trends in SOS and the smallest area with delaying trends for both meadow and steppe (Table S1). MODIS showed a larger area for advancing trends in SOS than for delaying trends. Both GIMMS3g (2001 to 2013) and SeaWiFS (1998 to 2006) had similar land areas for pixels with advancing and delaying trends in SOS, while GIMMS (1998 to 2006) had a larger area for pixels with advancing trends than for pixels with delaying trends.

3.3. Evaluating NDVI-Derived SOS With In Situ Measurements

We compared the SOS retrieved from the satellite-derived NDVI records with gross primary productivity (GPP) data from six eddy covariance flux sites and phenology observations from 15 sites across the plateau. The GPP data of the eddy covariance flux sites clearly showed the trajectories of plant growth and the phenological stages. The SOS retrieved from the remotely sensed data was generally close to the date when GPP exceeded 1 $gC/m^2/d$ during spring (Figure 5). The symbols above and below the dotted line GPP = 0 stand for the SOS based on the logistic and polynomial methods, respectively. At the Dan site where GPP was much lower than that of other three sites, the SOS retrieved from NDVI had larger differences among different data sets than other sites. The SOS for the five NDVI data sets based on the polynomial method had a larger range than that based on the logistic method. The root-mean-square error (RMSE) between NDVI-derived SOS and GPP-derived SOS varied from 9 days to 16 days for different data sets and methods (Figure 6). GIMMS3g and GIMMS had the largest RMSE, followed by MODIS; SPOT-VEG and SeaWiFS showed the lowest RMSE (Figure 6). The logistic method led to smaller RMSE than the polynomial method (Figure 6).

Conventional in situ phenology measurements are based on the development stages of plants at the species level, such as budburst or leaf-unfolding date. In situ phenology is different from the land surface phenology estimated from remote sensing data. Thus, these ground-based budburst data were used to evaluate the trends in spring phenology derived from NDVI data rather than to validate the SOS retrieved from NDVI. In situ phenology measurements were limited, and only 15 sites had data records over 7 years. Seven of the

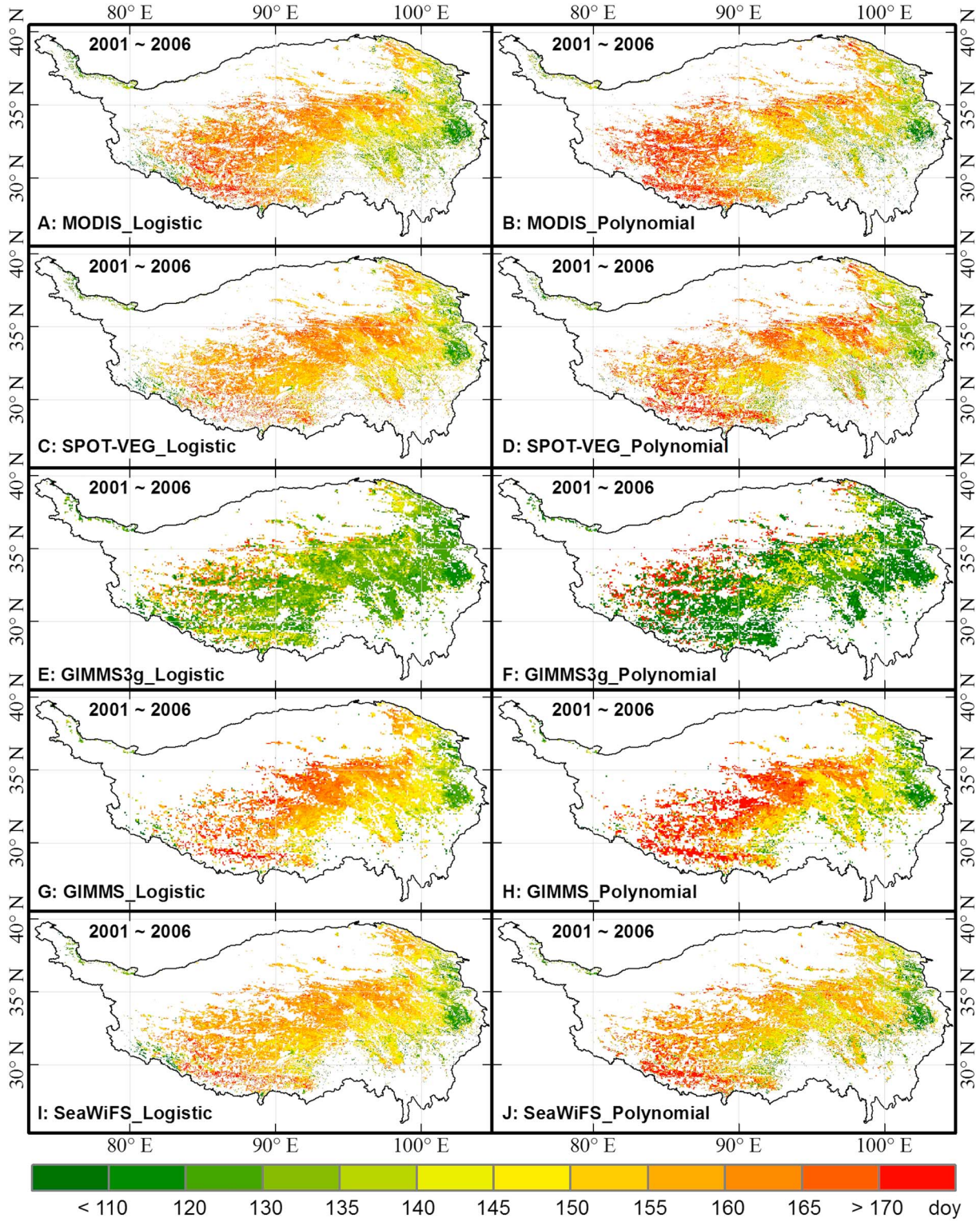

Figure 3. Spatial distribution of mean SOS during the period from 2001 to 2006 retrieved from the five NDVI data sets on the Tibetan plateau (only SOS in meadow and steppe area were retrieved according to the vegetation type data).

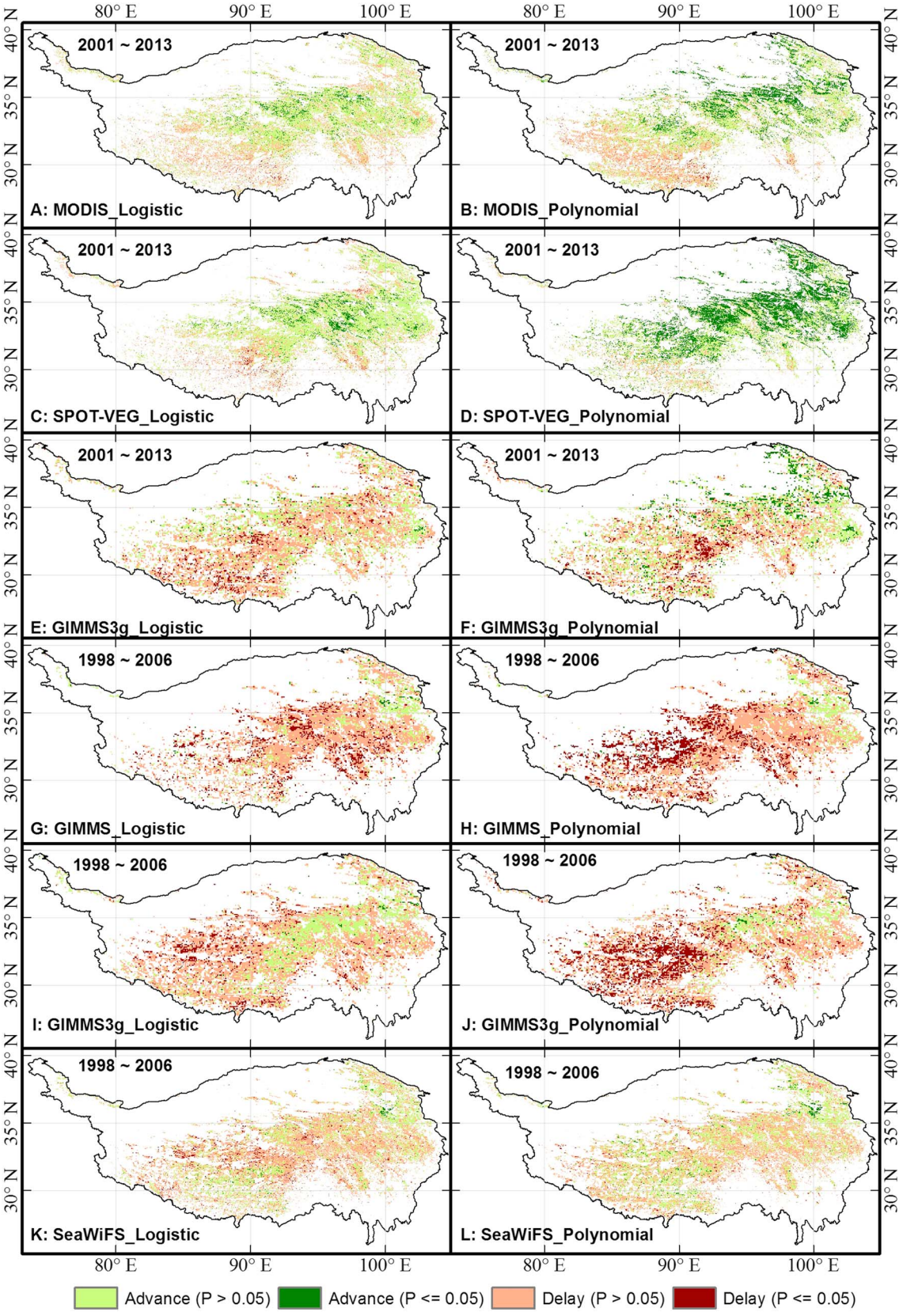

Figure 4. The trends in SOS retrieved from the five NDVI data sets based on both logistic and polynomial methods. The period from 2001 to 2013 was used for the MODIS, SPOT-VEG, and GIMMS3g data sets, and the period from 1998 to 2006 was used for the SeaWiFs, GIMMS3g, and GIMMS data sets.

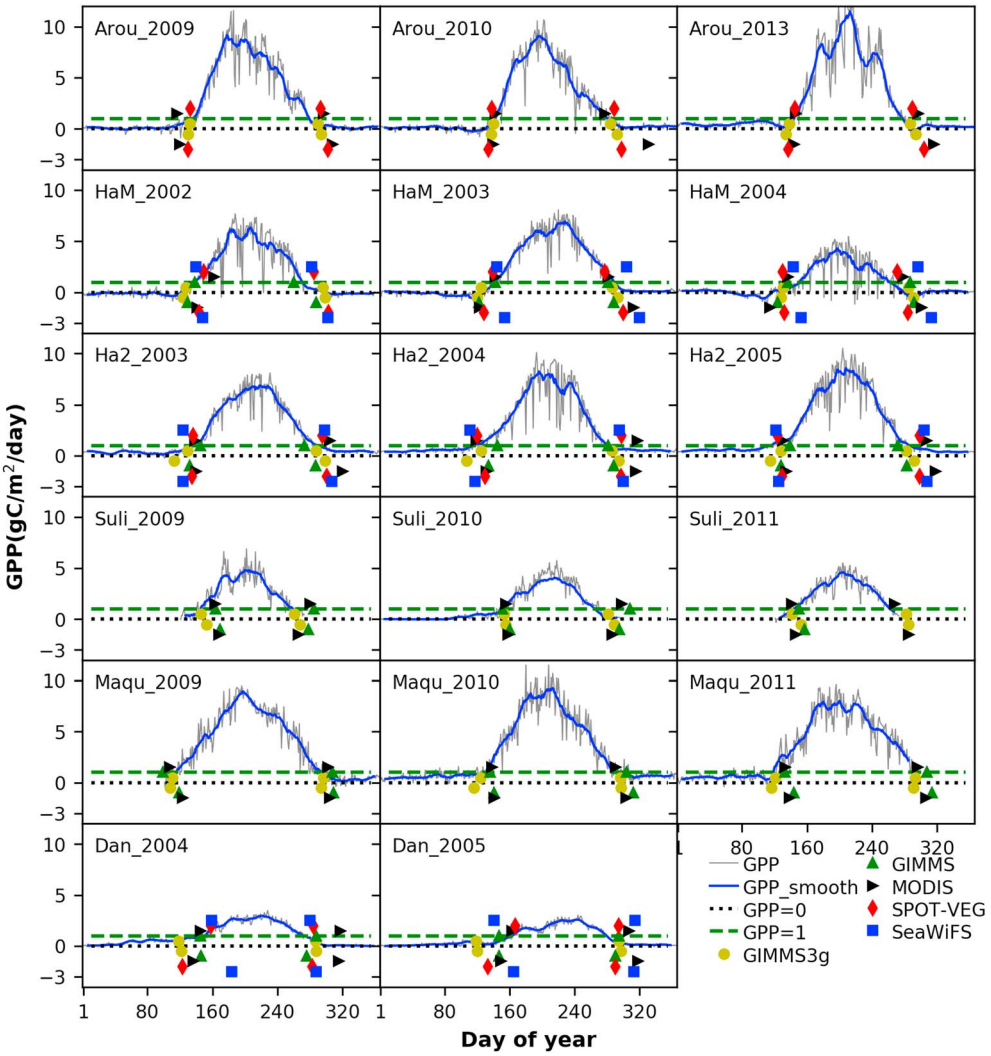

Figure 5. Evaluating the SOS retrieved from the five NDVI data sets based on the two retrieval methods using GPP data from eddy covariance flux sites. The symbols above the dotted line GPP = 0 stand for the SOS based on the logistic method, while the symbols below the dotted line GPP = 0 stand for the SOS based on the polynomial method.

15 sites are grassland, and eight of them are cropland sites. Most of the grassland sites are located in the meadow area, and only two of the seven grassland sites showed significant ($P < 0.05$) advancing SOS trend (Figure 7 and Table S2). All cropland sites exhibited insignificant advancing or delaying trends (Figure 7 and Table S2). The trends in the in situ phenology observations were greatly different from remote sensing retrieved SOS trends at all the 15 sites (Table S2). At the sites with significant advancing SOS trends from in situ phenology measurements, no advancing SOS trend was found from any of the five NDVI data set (Table S2).

3.4. Effects of Environmental Factors on SOS

To examine the environmental controls on spring phenology, we used air temperature, soil temperature at 0 cm, precipitation, and snow depth to analyze their controlling effects on SOS (Figure 8). Air temperature and soil temperature had the strongest relationships with SOS (R^2 ranging from 0.24 to 0.49 and from 0.18 to 0.49, respectively) among these environmental factors. Winter air temperature, spring air temperature, and the difference between spring and winter air temperature were used to analyze the effects of air temperature on SOS (Table S3). For each NDVI data set, the SOS showed different relationships with air temperature between the two retrieval methods. The SOS based on the polynomial method showed higher R^2 (ranging from 0.15 for GIMMS to 0.41 for SeaWiFS) with spring air temperature than with winter air

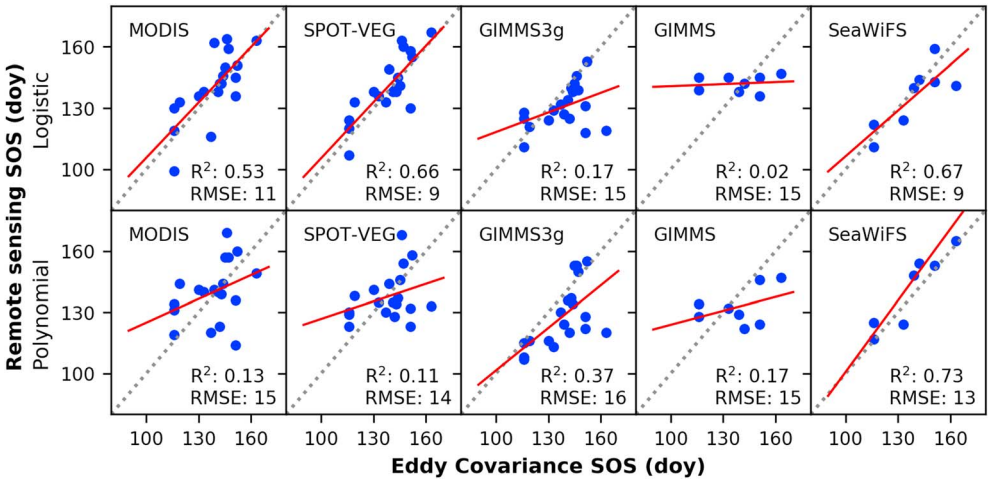

Figure 6. Comparison between SOS derived from remote sensing data sets and SOS derived from eddy covariance GPP data.

temperature or temperature difference between spring and winter for each data set. By contrast, the SOS based on the logistic method showed higher R^2 (ranging from 0.22 for MODIS to 0.49 for SeaWiFS) with temperature difference between spring and winter than with spring temperature or winter temperature for each data set.

Spring soil temperature, winter soil temperature, and the difference between spring and winter soil temperature were used to analyze the effects of soil temperature on SOS (Table S3). The SOS based on the polynomial method had the strongest relationships with spring soil temperature, with R^2 ranging from 0.16 (GIMMS) to 0.52 (SPOT-VEG). The SOS based on the logistic method had the strongest relationships with soil temperature difference between spring and winter for each NDVI data set, ranging from 0.18 (MODIS) to 0.45 (SeaWiFS).

The effects of precipitation on SOS were analyzed using winter precipitation, spring precipitation, and preseason precipitation (sum of winter and spring precipitation). Overall, the SOS on the Tibetan Plateau was poorly explained by precipitation, and the R^2 value was lower than 0.20 except for the relationship between spring precipitation and SOS based on the logistic method for SeaWiFS (R^2 = 0.38) (Table S3).

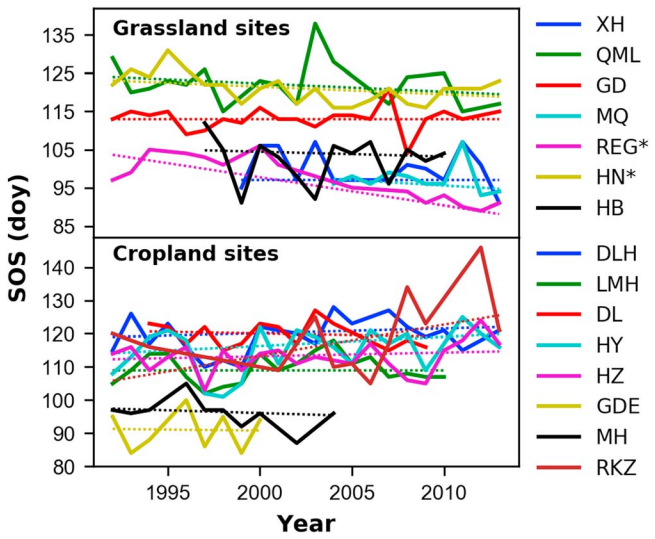

Figure 7. In situ SOS observations and their trends. The slope of the trend and *P* value for each site are shown in Table S2. The 15 sites are as follows: XH: Xinghai, QML: Qumalai, GD: Gande, MQ: Maqu, REG: Ruoergai, HN: Henan, HB: Haibei, DLH: Delingha, LMH: Luomuhong, HY: Huangyuan, HZ: Huzhu, GDE: Guide, MH: Minhe, RKZ: Rikeze. The two sites marked with asterisk (REG and HN) exhibited significant trends in SOS, while all other sites had insignificant trends.

The effects of snow on SOS were analyzed using spring snow depth, winter snow depth, and preseason snow depth (sum of winter and spring snow depth). Based on correlation analysis, the SOS on the Tibetan Plateau based on the polynomial method was poorly explained by snow depth with R^2 values lower than 0.15. The SOS based on the logistic method also had weak relationships with snow depth, and the R^2 value was lower than 0.20 for all data sets except for SeaWiFS and GIMMS with the logistic method (Table S3).

To examine the relative effects of environmental variables, we also performed partial correlation analysis between SOS and environmental factors. The partial correlation coefficients are shown in Table S4. The partial correlation coefficient varied greatly with SOS retrieval method. Among these environmental factors, soil temperature showed higher partial correlation coefficients than others. Among these data sets, SOS estimated from MODIS and SeaWiFS showed higher partial correlation than other data sets. Polynomial method-based SOS showed higher correlation coefficients than logistic method. The partial correlation analysis allowed us to determine the relative effects of multiple environmental factors on SOS. We also compared the trends of environmental factors with those of SOS estimated from the remote

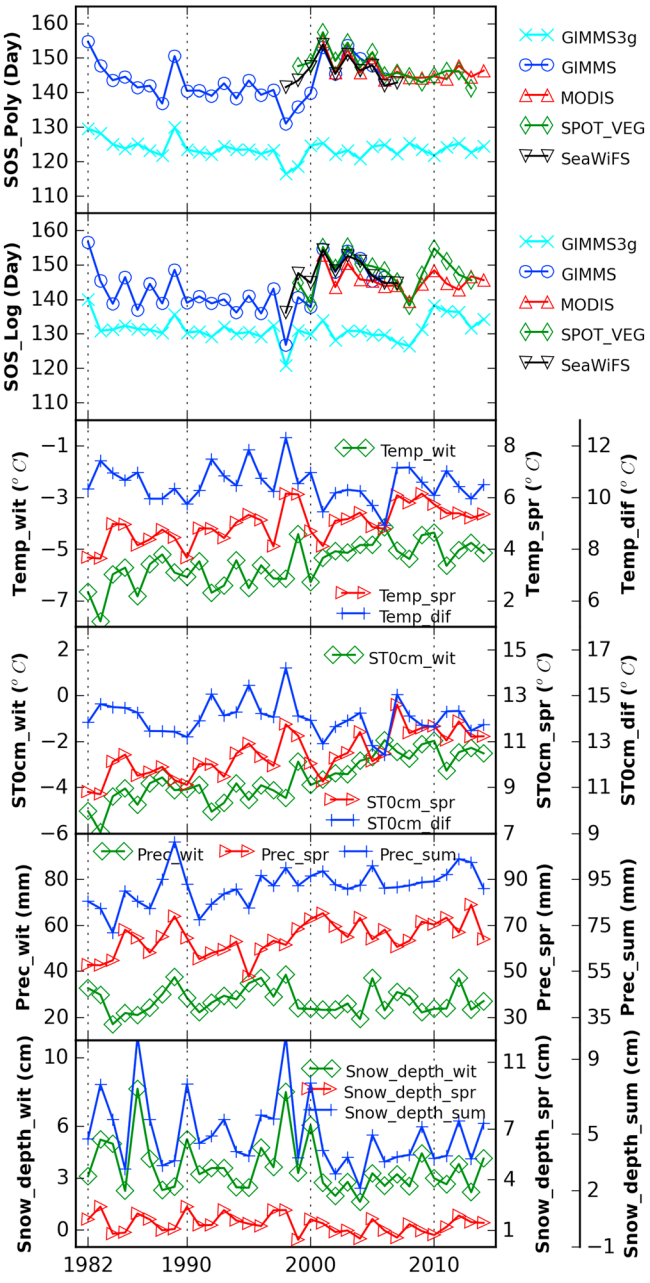

Figure 8. Yearly SOS derived using both polynomial and logistic methods, air temperature, soil 0 cm temperature, precipitation, and snow depth on the Tibetan Plateau from 1982 to 2014.

sensing data sets during the same period (Table S5). Soil temperature, air temperature, and precipitation exhibited significant increasing trends. Soil temperature increased faster than air temperature, and winter temperature increased faster than spring temperature. Snow depth exhibited a significant decreasing trend.

4. Discussion

Our results indicate no consistent trends in spring phenology among the different long-term satellite-derived NDVI records and between the two different SOS retrieval methods. The ground-based phenological observations demonstrated that only two of the 17 sites exhibited advancing trends in SOS. A recent study examined the SOS of an alpine shrub site on the Tibetan Plateau using 10 years of eddy covariance GPP data and found that there was no significant trend in SOS (Li et al., 2016). Our analyses revealed that the trends in spring phenology differed with satellite record and also varied with retrieval method. The debate on the trends in spring phenology on the Tibetan Plateau could be attributed to the use of different data sets and/or different SOS retrieval methods. Yu et al. (2010) reported that the SOS advanced from 1982 to mid-1990s and retreated after mid-1990s based on GIMMS data set, and this was not supported by our results based on the GIMMS3g data set. Zhang et al. (2013) argued that the SOS derived from GIMMS continuously advanced from 1982 to 1998 and then delayed from 1998 to 2006, while the SOS from MODIS and SPOT-VEG showed advancing trends from 1998 to 2006. Our results showed that the SOS retrieved from GIMMS after 2000 showed high consistency with that from MODIS, SPOT, and SeaWiFS and did not continue the advancing trend found in GIMMS SOS from 1982 to 1998. The inconsistency between the findings of Zhang et al. (2013) and our results likely resulted from the differences in processing the NDVI data. Shen et al. (2014) reported that there was no significant SOS trend from 2000 to 2011, and the SOS derived from GIMMS3g data set was greatly different from MODIS and SPOT data sets, which is consistent with our results. Different fitting methods in remote sensing phenology retrieving algorithm can lead to significantly different land surface phenology estimation (Wu et al., 2017).

The discrepancies in the SOS trends among different long-term satellite data sets could be partly attributed to the differences in the magnitude and trends in NDVI among these data sets. We compared the spatial patterns (Figure S3), histograms (Figure S4), and trends (Figure S5) of these five NDVI data sets on the Tibetan Plateau for different timescales (seasonal, growing season, and annual). For each timescale, the average NDVI was used for the calculation of the trend. SPOT-VEG showed significant increasing trends in NDVI for all timescales from 1999 to 2013 (Figure S5 and Table S6). No other data set showed significant increasing NDVI during spring. Guay et al. (2014) compared these five NDVI data sets in northern high latitudes and found that only 40% of the region showed similar trends in NDVI among these data sets. In cold regions, a break was detected in the NDVI trend of GIMMS3g in 2008, and no break was detected in the trends of MODIS and SPOT-VEG data (Tian et al., 2015). The NDVI correlation analysis among these data sets in different seasons indicated that MODIS, SPOT-VEG, and SeaWiFS showed high consistence; NDVI in meadow area showed higher consistence than that in steppe area; and spring NDVI showed lower consistence than winter, summer, and autumn NDVI. These results show that there was no consistency even for the NDVI trend on the Tibetan Plateau among different long-term NDVI records. The discrepancies in the NDVI data sets had large impacts on the retrieval of SOS. The substantial discrepancies in the NDVI trend could lead to large differences in the trend of SOS among NDVI data sets.

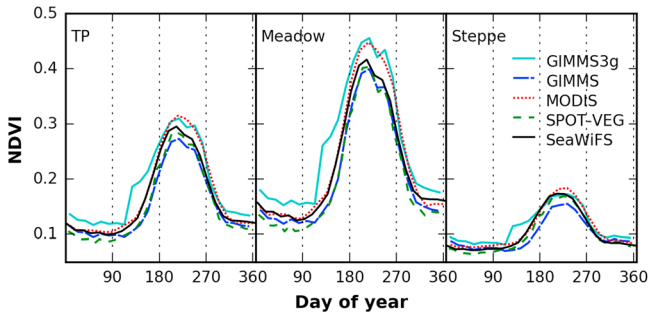

Figure 9. NDVI seasonal change curves of the five NDVI data sets on the Tibetan plateau (using the multiyear average from 2001 to 2006).

The discrepancies in SOS among the NDVI data sets were also partly caused by the differences in the quality of these data sets. Each NDVI data set contains noise caused by a variety of factors such as cloud, snow, aerosol, topography, and sensor calibration. These noise can lead to large changes in the SOS estimates (Yi & Zhou, 2011). The NDVI of GIMMS3g was systematically higher than that of other data sets for both meadow and steppe areas in winter and spring (Figures S5 and 9). During spring, GIMMS3g NDVI started increasing earlier than other four data sets and also had an abrupt change. As a result, the SOS retrieved from GIMMS3g was systematically lower (or earlier) than that from other data sets.

To test the sensitivity of spring phenology to NDVI noise, a 30% random noise was added to the regionally averaged MODIS NDVI time series. The sensitivity of SOS was assessed using the difference between the SOS results based on NDVI without the addition of random noise and an ensemble (size = 50) average SOS based on NDVI with 30% random noise (Figure 10). The 3 day error in SOS could be resulted from the addition of 30% noise in one NDVI value in one year. For the polynomial method, the noise in NDVI around the SOS date had large impact on the retrieval of SOS. For the logistic method, both NDVI around the SOS date and peak growing season had large impact on the estimation of SOS. The positive and negative noise around SOS date would lead to underestimation and overestimation of SOS, respectively. By contrast, the positive and negative noise around the peak growing season would lead to overestimation and underestimation of SOS, respectively.

We also analyzed the quality control (QC) flag of the MODIS and SPOT-VEG data sets from 2001 to 2013 (Figure S6). Snow contamination was the main reason for the low quality of NDVI during the nongrowing season, while other factors such as cloud, topography, and aerosol were mainly responsible for the low quality of NDVI during the growing season. During spring when SOS was sensitive to noise in NDVI, the number of pixels contaminated by snow and other factors were equivalent to each other. GIMMS3g does not separate snow and other factors in its QC flag. In the meadow area, a large number of pixels between Julian day 100 and 180 for the GIMMS3g were filled using spline interpolation, which is likely responsible for the abrupt changes in NDVI during spring. Our results indicate that further improving the quality of the long-term NDVI data sets could lead to better estimates of SOS and better understanding of phenology responses to environmental change.

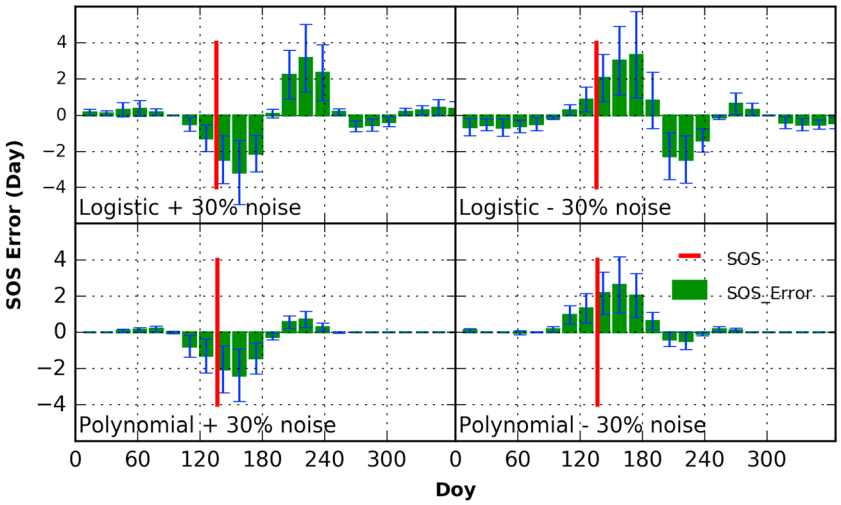

Figure 10. Sensitivity analysis of SOS error based on both polynomial and logistic methods to noise in a NDVI value for each day of the year (DOY). The green bars stand for the mean SOS error of the ensemble, and the error bars stand for the standard deviation of SOS error. The red line is the SOS (DOY) estimated with NDVI curve without noise.

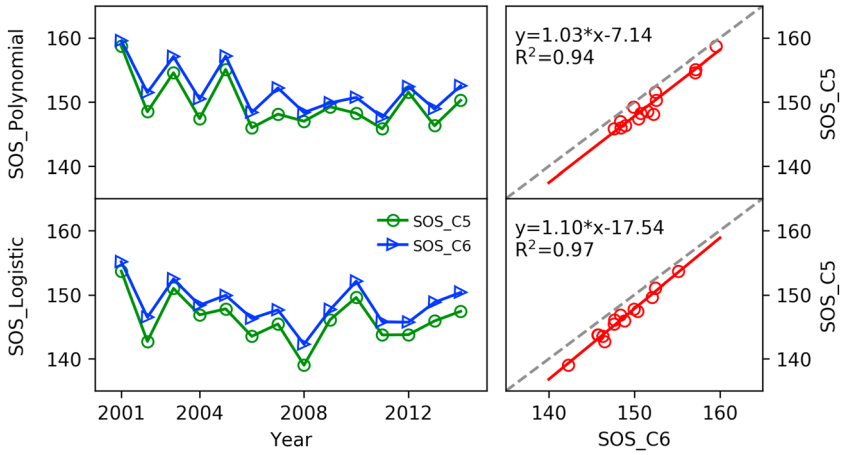

Figure 11. Comparison of SOS estimated from the MODIS NDVI Collection 5 (C5) data set and the MODIS NDVI Collection 6 data set (C6).

Our results indicate that SPOT-VEG, MODIS, and SeaWiFS had higher accuracy in phenology estimation and are more appropriate for examining the trends in SOS on the Tibetan Plateau than GIMMS and GIMMS3g. Although GIMMS and GIMMS3g data have longer duration than other NDVI data sets, their lower accuracy in SOS estimation on the Tibetan Plateau could result in larger uncertainties in the SOS trend. The data quality of the NDVI data sets had significant effects on SOS estimation. For example, GIMMS3g and GIMMS are both based on AVHRR data but with different processing procedures, and the SOS estimated from these two data sets exhibited large differences. We also compared the SOS retrieved from MODIS NDVI Collection 5 (C5) and that from MODIS NDVI Collection 6 (C6). The SOS based on C6 NDVI was systematically higher than that based on C5 NDVI (Figure 11). The SOS derived from carbon flux data was used to evaluate the SOS derived from both C5 and C6 MODIS NDVI. The C5 NDVI had slightly higher accuracy in SOS estimation than the C6 NDVI (Figure S7).

We used the flux tower GPP to evaluate the SOS derived from the NDVI data sets and used the field phenological observations to examine and evaluate the trends in SOS. It should be noted that there is a scale mismatch between remote sensing pixels and footprints of field sites (e.g., eddy covariance flux towers). The pixel size of the NDVI data sets, particularly GIMMS and GIMMS (8 km), is typically larger than the footprint of an eddy covariance flux tower. Moreover, a pixel is of a fixed size for a specific sensor, while the footprint of an eddy covariance flux tower varies with wind speed, wind direction, tower height, and surface roughness (Kljun et al., 2015). To examine the representativeness of each flux site and assess the scale mismatch between its footprint and the NDVI pixels, we calculated the fractional cover of grassland within the 1 km × 1 km and 8 km × 8 km windows surrounding the tower. The fractional cover of grassland was close to 1.0 for all sites except Maqu. This indicates that using flux tower GPP to evaluate the SOS derived from the NDVI data sets was reasonable to some extent despite the scale mismatch. The field phenological observations for a given site were based on a specific species, while the pixel in which the site is located consists of multiple vegetation types and/or multiple species. Although in situ measurements have been widely used to evaluate phenology derived from satellite data (Coops et al., 2007; Turner et al., 2003), the scale mismatch can result in significant discrepancies in spring phenology between in situ measurements and satellite observations (Chen et al., 2008). In addition, the smoothing of daily GPP using the 15 day moving window could also introduce uncertainty to the derived SOS.

Our findings have implications for terrestrial biosphere modeling. Phenology representation is an important part of terrestrial biosphere models and has fundamental impacts on simulated water, carbon, and energy exchange (Richardson et al., 2012; Xin et al., 2015). The evaluation of multiple long-term NDVI records and different methods for phenology retrieval can shed light on the reliability of the NDVI records and the resulting phenology estimates. Phenology is prescribed in diagnostic terrestrial biosphere models, and the evaluation of remote sensed based phenology can help assess the effects of prescribed phenology on modeled carbon, water, and energy dynamics and reduce the uncertainty in terrestrial biosphere modeling. Accurate satellite-derived phenology products can also be used to validate simulated phenology and/or

calibrate parameters for prognostic terrestrial biosphere models (Xin, 2016; Xin et al., 2015). In a number of modeling studies, long-term satellite data from one sensor have been used to evaluate the models or calibrate the parameters (Forkel et al., 2014; Knorr et al., 2010; Macbean et al., 2015; Stöckli et al., 2011). Our results indicate that multiple satellite data sets rather than one of them should be used to evaluate or calibrate models; alternatively, the range of multiple data sets could provide uncertainty estimates that can be used for model evaluation or parameter estimation.

The SOS was affected by a number of environmental factors, such as air temperature, precipitation, snow, and soil temperature. Some factors had positive effects, and some had negative effects. Even for a given factor, it could have opposite effects on SOS in different seasons. Air temperature is one of the most important factors controlling SOS in alpine ecosystems (Jeong et al., 2009; Piao et al., 2011; Zhang et al., 2015), particularly in high elevation areas of the Tibetan Plateau (Liu et al., 2014). Spring air temperature was considered as the main factor controlling the spring phenology on the Tibetan Plateau (Shen, 2011). Air temperature increase in spring could advance SOS, but air temperature increase in winter could delay SOS because of the failure of plants to fulfill chilling (Zhang et al., 2013). In the last three decades on the Tibetan Plateau, winter air temperature (0.053°C/yr, $P<0.0001$) increased slightly faster than spring air temperature (0.046°C/yr, $P<0.0001$). The air temperature difference between spring and winter showed a decreasing trend that was not statistically significant (rate = −0.008°C/yr; $P = 0.45$). The soil temperature at 0 cm increased at a higher rate than air temperature, with winter and spring soil temperature increasing at rates of 0.08°C/yr ($P<0.0001$) and 0.079°C/yr ($P<0.0001$), respectively. The offsetting effects of spring temperature and winter temperature could result insignificant trends in SOS on the plateau. The partial correlation analysis showed that spring and winter temperature had opposite effects on SOS for some data sets (e.g., soil temperature and SOS estimated from SeaWiFS with polynomial method). Precipitation is another important environmental factor controlling SOS on the Tibetan Plateau. Cumulative precipitation in spring and preseason increased significantly at rates of 0.38 mm/yr ($P = 0.003$) and 0.04 mm/yr ($P = 0.007$) from 1982 to 2014, respectively. Increasing evapotranspiration resulting from climate warming will intensify the surface moisture stress on the Tibetan Plateau, while spring precipitation can relieve this stress (Shen et al., 2014; Zhang et al., 2015). Winter snow had a large impact on the SOS of grasslands (Yu et al., 2013). Snow melting can amplify or dampen the effect of climate warming (Suzuki, 2014). During the last three decades, winter snow depth, spring snow depth, and preseason snow depth (the sum of spring snow depth and winter snow depth) decreased at rates of −0.97 cm/yr ($P = 0.051$), −0.65 cm/yr ($P = 0.001$), and −1.51 cm/yr ($P = 0.016$), respectively. The Tibetan Plateau covers a land area of $2{,}542.30 \times 10^3$ km^2, and the effects of the environmental factors on SOS could vary with latitude, longitude, and elevation because of different water supply, heat conditions, and soil properties (Liu et al., 2016).

5. Conclusions

There were large discrepancies in the magnitude, spatial patterns, and long-term trends in the SOS among different satellite-derived NDVI data sets and between different retrieval methods. This finding indicates that the discrepancies in the trends of spring phenology over the Tibetan Plateau among different studies could be largely attributed to the use of different NDVI data sets and/or different phenology retrieval methods. Our results therefore can help settle the debate on the trends of spring phenology over the Tibetan Plateau. Our results demonstrate that there were no consistent trends in spring phenology for alpine meadow and steppe over the Tibetan Plateau. The in situ budburst data also indicated no significant trends in spring phenology. The discrepancies in SOS among the different NDVI data sets mainly resulted from the differences in the magnitude and trends of the NDVI data; the noise of the data sets caused by snow, cloud, and other factors; and the different SOS retrieval methods. The relationships between SOS and environmental factors (air temperature, precipitation, soil temperature, and snow depth) also varied with NDVI data set and retrieval method. The correlation analysis between SOS and environmental factors showed that the increases in winter and spring temperature had offsetting effects on spring phenology.

Acknowledgments

This work was supported by China's funding agencies (the National Natural Science Foundation of China grants 91425303 and 41771466, China Postdoctoral Science Foundation grant 2015T81067, and China Scholarship Council) and the U.S. funding agencies (National Aeronautics and Space Administration (NASA) through the Carbon Cycle Science Program grant NNX14AJ18G and National Science Foundation (NSF) through MacroSystems Biology grants EF-1065777 and EF-1638688). We thank HiWATER, CERN, China Meteorological Administration (CMA), and FLUXNET for providing data. We also thank Yongjian Ding, Jia Qin, and Xiaoyun Wang for their help with flux data collection. Summaries of the data used in this study can be found in the supporting information. Full data sets and code used in this study are available at UNH's Global Ecology Group website: http://globalecology.unh.edu/data.html or by contacting Xufeng Wang (wangxufeng@lzb.ac.cn). More details about accessing the data sets used in this study are provided in supporting information. We thank the two anonymous reviewers for their constructive comments on the manuscript. X. F. Wang and J. F. Xiao designed research; X. F. Wang and J. F. Xiao performed research; T. Che, L. Y. Dai, S. Y. Wang, and J. K. Wu contributed data; X. F. Wang and J. F. Xiao analyzed data; X. F. Wang and J. F. Xiao wrote the paper; and X. Li, G. D. Cheng, and M.G. Ma provided comments and suggestions on the manuscript.

References

Badeck, F. W., Bondeau, A., Bottcher, K., Doktor, D., Lucht, W., Schaber, J., & Sitch, S. (2004). Responses of spring phenology to climate change. *The New Phytologist*, *162*, 295–309. https://doi.org/10.1111/j.1469-8137.2004.01059.x

Balzarolo, M., Vicca, S., Nguy-Robertson, A. L., Bonal, D., Elbers, J. A., Fu, Y. H., … Veroustraete, F. (2016). Matching the phenology of Net Ecosystem Exchange and vegetation indices estimated with MODIS and FLUXNET in-situ observations. *Remote Sensing of Environment*, *174*, 290–300. https://doi.org/10.1016/j.rse.2015.12.017

Chen, B., Chen, J. M., Mo, G., Black, T. A., & Worthy, D. E. (2008). Comparison of regional carbon flux estimates from CO_2 concentration measurements and remote sensing based footprint integration. *Global Biogeochemical Cycles*, *22*, GB2012. https://doi.org/110.1029/2007GB003024

Chen, X., An, S., Inouye, D. W., & Schwartz, M. D. (2015). Temperature and snowfall trigger alpine vegetation green-up on the world's roof. *Global Change Biology*, *21*(10), 3635–3646.

China Meteorological Administration (1993). *Standard specification for agricultural meteorological observation (I)*. Beijing: China Meteorological Press.

Coops, N. C., Black, T. A., Jassal, R. S., Trofymow, J. A., & Morgenstern, K. (2007). Comparison of MODIS, eddy covariance determined and physiologically modelled gross primary production (GPP) in a Douglas-fir forest stand. *Remote Sensing of Environment*, *107*, 385–401. https://doi.org/10.1016/j.rse.2006.09.010

Dai, L., Che, T., & Ding, Y. (2015). Inter-calibrating SMMR, SSM/I and SSMI/S data to improve the consistency of snow-depth products in China. *Remote Sensing*, *7*(6), 7212.

Deronde, B., Debruyn, W., Gontier, E., Goor, E., Jacobs, T., Verbeiren, S., & Vereecken, J. (2014). 15 years of processing and dissemination of SPOT-VEGETATION products. *International Journal of Remote Sensing*, *35*(7), 2402–2420.

Didan, K., Munoz, A. B., Solano, R., & Huete, A. (2015). MODIS vegetation index user's guide (MOD13 series) version 3.00, June 2015 (Collection 6).

Ding, M. J., Li, L. H., Nie, Y., Chen, Q., & Zhang, Y. L. (2016). Spatio-temporal variation of spring phenology in Tibetan Plateau and its linkage to climate change from 1982 to 2012. *Journal of Mountain Science*, *13*(1), 83–94. https://doi.org/10.1007/s11629-015-3600-0

Duan, A. M., & Xiao, Z. X. (2015). Does the climate warming hiatus exist over the Tibetan Plateau? *Scientific Reports*, *5*, 13711. https://doi.org/10.1038/srep13711

Forkel, M., Migliavacca, M., Reichstein, M., Schaphoff, S., Thonicke, K., Thurner, M., … Carvalhais, N. (2014). Identifying controls on vegetation greenness phenology through model-data integration. *Biogeosciences*, *11*(23), 7025–7050.

Fu, Y. S. H., Zhao, H., Piao, S., Peaucelle, M., Peng, S., Zhou, G., … Janssens, I. A. (2015). Declining global warming effects on the phenology of spring leaf unfolding. *Nature*, *526*(7571), 104–107. https://doi.org/10.1038/nature15402

Ganjurjav, H., Gao, Q., Zhang, W., Liang, Y., Li, Y., Cao, X., … Danjiu, L. (2015). Effects of warming on CO(2) fluxes in an alpine meadow ecosystem on the Central Qinghai–Tibetan Plateau. *PLoS One*, *10*(7), e0132044. https://doi.org/10.1371/journal.pone.0132044

Guay, K. C., Beck, P. S. A., Berner, L. T., Goetz, S. J., Baccini, A., & Buermann, W. (2014). Vegetation productivity patterns at high northern latitudes: A multi-sensor satellite data assessment. *Global Change Biology*, *20*(10), 3147–3158. https://doi.org/10.1111/gcb.12647

Guo, L. Y., Wu, Z. N., & Chun, T. H. (2011). Impacts of climatic warming on reproductive stages of forages growing in alpine grassland of the Three River Sources Areas. *Pratacultural Science*, *04*, 8.

Holben, B. N. (1986). Characteristics of maximum-value composite images from temporal AVHRR data. *International Journal of Remote Sensing*, *7*(11), 1417–1434. https://doi.org/10.1080/01431168608948945

Hou, X. (2001). *1:1000,000 Vegetation Atlas of China, Editorial Board of Vegetation Map of China CAS*. Beijing, China: Science Press.

Huete, A., Didan, K., Miura, T., Rodriguez, E. P., Gao, X., & Ferreira, L. G. (2002). Overview of the radiometric and biophysical performance of the MODIS vegetation indices. *Remote Sensing of Environment*, *83*(1–2), 195–213. https://doi.org/10.1016/S0034-4257(02)00096-2

Jeong, S. J., Ho, C. H., & Jeong, J. H. (2009). Increase in vegetation greenness and decrease in springtime warming over east Asia. *Geophysical Research Letters*, *36*, L02710. https://doi.org/10.1029/2008GL036583

Julien, Y., & Sobrino, J. A. (2009). Global land surface phenology trends from GIMMS database. *International Journal of Remote Sensing*, *30*, 3495–3513. https://doi.org/10.1080/01431160802562255

Justice, C. O., Vermote, E., Townshend, J. R. G., Defries, R., Roy, D. P., Hall, D. K., … Barnsley, M. J. (1998). The Moderate Resolution Imaging Spectroradiometer (MODIS): Land remote sensing for global change research. *IEEE Transactions on Geoscience and Remote Sensing*, *36*(4), 1228–1249. https://doi.org/10.1109/36.701075

Kljun, N., Calanca, P., Rotach, M. W., & Schmid, H. P. (2015). A simple two-dimensional parameterisation for Flux Footprint Prediction (FFP). *Geoscientific Model Development*, *8*(11), 3695–3713. https://doi.org/10.5194/gmd-8-3695-2015

Knorr, W., Kaminski, T., Scholze, M., Gobron, N., Pinty, B., Giering, R., & Mathieu, P. P. (2010). Carbon cycle data assimilation with a generic phenology model. *Journal of Geophysical Research*, *115*, G04017. https://doi.org/10.1029/2009JG001119

Lasslop, G., Reichstein, M., Papale, D., Richardson, A. D., Arneth, A., Barr, A., … Wohlfahrt, G. (2010). Separation of net ecosystem exchange into assimilation and respiration using a light response curve approach: Critical issues and global evaluation. *Global Change Biology*, *16*, 187–208.

Li, H. Q., Zhang, F. W., Li, Y. N., Wang, J. B., Zhang, L. M., Zhao, L., … Du, M. Y. (2016). Seasonal and inter-annual variations in CO_2 fluxes over 10 years in an alpine shrubland on the Qinghai-Tibetan Plateau, China. *Agricultural and Forest Meteorology*, *228*, 95–103. https://doi.org/10.1016/j.agrformet.2016.06.020

Li, X., Cheng, G., Liu, S., Xiao, Q., Ma, M., Jin, R., … Xu, Z. (2013). Heihe Watershed Allied Telemetry Experimental Research (HiWATER): Scientific objectives and experimental design. *Bulletin of the American Meteorological Society*, *94*(8), 1145–1160. https://doi.org/10.1175/Bams-D-12-00154.1

Li, X., Li, X., Li, Z., Ma, M., Wang, J., Xiao, Q., … Yan, G. (2009). Watershed allied telemetry experimental research. *Journal of Geophysical Research*, *114*, D22103. https://doi.org/10.1029/2008JD011590

Liu, L. L., Liu, L. Y., Liang, L., Donnelly, A., Park, I., & Schwartz, M. D. (2014). Effects of elevation on spring phenological sensitivity to temperature in Tibetan Plateau grasslands. *Chinese Science Bulletin*, *59*(34), 4856–4863. https://doi.org/10.1007/s11434-014-0476-2

Liu, L. L., Zhang, X. Y., Donnelly, A., & Liu, X. J. (2016). Interannual variations in spring phenology and their response to climate change across the Tibetan Plateau from 1982 to 2013. *International Journal of Biometeorology*. https://doi.org/10.1007/s00484-016-1147-6

Macbean, N., Maignan, F., Peylin, P., Bacour, C., Bréon, F. M., & Ciais, P. (2015). Using satellite data to improve the leaf phenology of a global terrestrial biosphere model. *Biogeosciences*, *12*(12), 13311–13373.

McClain, C. R., Feldman, G. C., & Hooker, S. B. (2004). An overview of the SeaWiFS project and strategies for producing a climate research quality global ocean bio-optical time series. *Deep Sea Research Part II: Topical Studies in Oceanography*, *51*, 5–42. https://doi.org/10.1016/j.dsr2.2003.11.001

Menzel, A., Sparks, T. H., Estrella, N., Koch, E., Aasa, A., Ahas, R., … Zust, A. (2006). European phenological response to climate change matches the warming pattern. *Global Change Biology*, *12*, 1969–1976. https://doi.org/10.1111/j.1365-2486.2006.01193.x

Penuelas, J., Rutishauser, T., & Filella, I. (2009). Phenology feedbacks on climate change. *Science*, *324*(5929), 887–888. https://doi.org/10.1126/science.1173004

Piao, S., Cui, M., Chen, A., Wang, X., Ciais, P., Liu, J., & Tang, Y. (2011). Altitude and temperature dependence of change in the spring vegetation green-up date from 1982 to 2006 in the Qinghai-Xizang Plateau. *Agricultural and Forest Meteorology*, *151*, 1599–1608. https://doi.org/10.1016/j.agrformet.2011.06.016

Pinzon, J. E., & Tucker, C. J. (2014). A non-stationary 1981–2012 AVHRR NDVI3g time series. *Remote Sensing*, *6*(8), 6929–6960.
Reed, B. C., Brown, J. F., Vanderzee, D., Loveland, T. R., Merchant, J. W., & Ohlen, D. O. (1994). Measuring phenological variability from satellite imagery. *Journal of Vegetation Science*, *5*(5), 703–714. https://doi.org/10.2307/3235884
Richardson, A. D., Anderson, R. S., Arain, M. A., Barr, A. G., Bohrer, G., Chen, G., … Xue, Y. (2012). Terrestrial biosphere models need better representation of vegetation phenology: Results from the North American Carbon Program Site Synthesis. *Global Change Biology*, *18*, 566–584. https://doi.org/10.1111/j.1365-2486.2011.02562.x
Richardson, A. D., Andy Black, T., Ciais, P., Delbart, N., Friedl, M. A., Gobron, N., … Varlagin, A. (2010). Influence of spring and autumn phenological transitions on forest ecosystem productivity. *Philosophical Transactions of the Royal Society B*, *365*, 3227–3246. https://doi.org/10.1098/rstb.2010.0102
Richardson, A. D., Keenan, T. F., Migliavacca, M., Ryu, Y., Sonnentag, O., & Toomey, M. (2013). Climate change, phenology, and phenological control of vegetation feedbacks to the climate system. *Agricultural and Forest Meteorology*, *169*, 156–173. https://doi.org/10.1016/j.agrformet.2012.09.012
Sen, P. K. (1968). Estimates of regression coefficient based on Kendall'stau. *Journal of the American Statistical Association*, *63*, 11.
Shen, M. (2011). Spring phenology was not consistently related to winter warming on the Tibetan Plateau. *Proceedings of the National Academy of Sciences*, *108*, E91–E92. https://doi.org/10.1073/pnas.1018390108
Shen, M., Sun, Z., Wang, S., Zhang, G., Kong, W., Chen, A., & Piao, S. (2013). No evidence of continuously advanced green-up dates in the Tibetan Plateau over the last decade. *Proceedings of the National Academy of Sciences of the United States of America*, *110*(26), E2329–E2329. https://doi.org/10.1073/pnas.1304625110
Shen, M., Tang, Y., Chen, J., Zhu, X., & Zheng, Y. (2011). Influences of temperature and precipitation before the growing season on spring phenology in grasslands of the central and eastern Qinghai-Tibetan Plateau. *Agricultural and Forest Meteorology*, *151*, 1711–1722.
Shen, M. G., Zhang, G. X., Cong, N., Wang, S. P., Kong, W. D., & Piao, S. L. (2014). Increasing altitudinal gradient of spring vegetation phenology during the last decade on the Qinghai-Tibetan Plateau. *Agricultural and Forest Meteorology*, *189*, 71–80. https://doi.org/10.1016/j.agrformet.2014.01.003
Shi, P., Sun, X., Xu, L., Zhang, X., He, Y., Zhang, D., & Yu, G. (2006). Net ecosystem CO2 exchange and controlling factors in a steppe—Kobresia meadow on the Tibetan Plateau. *Science in China Series D: Earth Sciences*, *49*, 207–218.
Stöckli, R., Rutishauser, T., Baker, I., Liniger, M. A., & Denning, A. S. (2011). A global reanalysis of vegetation phenology. *Journal of Geophysical Research*, *116*, G03020. https://doi.org/10.1029/2010JG001545
Suzuki, R. O. (2014). Combined effects of warming, snowmelt timing, and soil disturbance on vegetative development in a grassland community. *Plant Ecology*, *215*(12), 1399–1408. https://doi.org/10.1007/s11258-014-0396-x
Tian, F., Fensholt, R., Verbesselt, J., Grogan, K., Horion, S., & Wang, Y. J. (2015). Evaluating temporal consistency of long-term global NDVI datasets for trend analysis. *Remote Sensing of Environment*, *163*, 326–340. https://doi.org/10.1016/j.rse.2015.03.031
Tucker, C. J., Pinzon, J. E., Brown, M. E., Slayback, D. A., Pak, E. W., Mahoney, R., … El Saleous, N. (2005). An extended AVHRR 8-km NDVI dataset compatible with MODIS and SPOT vegetation NDVI data. *International Journal of Remote Sensing*, *26*, 4485–4498. https://doi.org/10.1080/01431160500168686
Turner, D. P., Ritts, W. D., Cohen, W. B., Gower, S. T., Zhao, M., Running, S. W., … Munger, J. (2003). Scaling gross primary production (GPP) over boreal and deciduous forest landscapes in support of MODIS GPP product validation. *Remote Sensing of Environment*, *88*(3), 256–270.
Wang, S. Y., Zhang, Y., Lu, S. H., Su, P. X., Shang, L. Y., & Li, Z. G. (2016). Biophysical regulation of carbon fluxes over an alpine meadow ecosystem in the eastern Tibetan Plateau. *International Journal of Biometeorology*, *60*(6), 801–812. https://doi.org/10.1007/s00484-015-1074-y
Wang, T., Peng, S., Lin, X., & Chang, J. (2013). Declining snow cover may affect spring phenological trend on the Tibetan Plateau. *Proceedings of the National Academy of Sciences of the United States of America*, *110*(31), E2854–E2855. https://doi.org/10.1073/pnas.1306157110
Wang, X. F., Ma, M. G., Li, X., & Song, Y. (2013). Validation of MODIS-GPP product at 10 flux sites in northern China. *International Journal of Remote Sensing*, *34*(2), 587–599. https://doi.org/10.1080/01431161.2012.715774
Wu, C., Peng, D., Soudani, K., Siebicke, L., Gough, C. M., Arain, M. A., … Ge, Q. (2017). Land surface phenology derived from normalized difference vegetation index (NDVI) at global FLUXNET sites. *Agricultural and Forest Meteorology*, *233*, 171–182. https://doi.org/10.1016/j.agrformet.2016.11.193
Wu, J. K., Zhang, S. Q., Wu, H., Liu, S. W., Qin, Y., & Qin, J. (2015). Actual evapotranspiration in Suli alpine meadow in northeastern edge of Qinghai-Tibet Plateau, China. *Advances in Meteorology*. https://doi.org/10.1155/2015/593649
Xin, Q. (2016). A risk-benefit model to simulate vegetation spring onset in response to multi-decadal climate variability: Theoretical basis and applications from the field to the Northern Hemisphere. *Agricultural and Forest Meteorology*, *228*, 139–163.
Xin, Q., Broich, M., Zhu, P., & Gong, P. (2015). Modeling grassland spring onset across the Western United States using climate variables and MODIS-derived phenology metrics. *Remote Sensing of Environment*, *161*, 63–77.
Xu, W. X., Xin, Y. C., Zhang, J., Xiao, R. X., & W. X. M. (2014). Phenological variation of alpine grasses (Gramineae) in the northeastern Qinghai Tibetan Plateau, China during the last 20 years. *Acta Ecologica Sinica*, *34*(7), 14.
Yi, S. H., & Zhou, Z. Y. (2011). Increasing contamination might have delayed spring phenology on the Tibetan Plateau. *Proceedings of the National Academy of Sciences of the United States of America*, *108*, E94–E94. https://doi.org/10.1073/pnas.1100394108
Yu, H. Y., Luedeling, E., & Xu, J. C. (2010). Winter and spring warming result in delayed spring phenology on the Tibetan Plateau. *Proceedings of the National Academy of Sciences of the United States of America*, *107*, 22,151–22,156. https://doi.org/10.1073/pnas.1012490107
Yu, Z., Liu, S. R., Wang, J. X., Sun, P. S., Liu, W. G., & Hartley, D. S. (2013). Effects of seasonal snow on the growing season of temperate vegetation in China. *Global Change Biology*, *19*(7), 2182–2195. https://doi.org/10.1111/gcb.12206
Zhang, G. L., Zhang, Y. J., Dong, J. W., & Xiao, X. M. (2013). Green-up dates in the Tibetan Plateau have continuously advanced from 1982 to 2011. *Proceedings of the National Academy of Sciences of the United States of America*, *110*(11), 4309–4314. https://doi.org/10.1073/pnas.1210423110
Zhang, W. J., Yi, Y. H., Kimball, J. S., Kim, Y., & Song, K. C. (2015). Climatic controls on spring onset of the Tibetan Plateau Grasslands from 1982 to 2008. *Remote Sensing*, *7*(12), 16,607–16,622. https://doi.org/10.3390/rs71215847
Zhang, X., Sun, S., Yong, S., Zhou, Z., & Wang, R. (2007). *Vegetation map of the People's Republic of China (1: 1000000)*. House: *Geology Publishing*.
Zhang, X. Y., Friedl, M. A., Schaaf, C. B., Strahler, A. H., Hodges, J. C. F., Gao, F., … Huete, A. (2003). Monitoring vegetation phenology using MODIS. *Remote Sensing of Environment*, *84*(3), 471–475. https://doi.org/10.1016/s0034-4257(02)00135-9
Zhao, L., Li, Y., Xu, S., Zhou, H., Gu, S., Yu, G., & Zhao, X. (2006). Diurnal, seasonal and annual variation in net ecosystem CO_2 exchange of an alpine shrubland on Qinghai-Tibetan plateau. *Global Change Biology*, *12*, 1940–1953.
Zhao, L., Li, Y. N., Gu, S., Zhao, X. Q., Xu, S. X., & Yu, G. R. (2005). Carbon dioxide exchange between the atmosphere and an alpine shrubland meadow during the growing season on the Qinghai-Tibetan Plateau. *Journal of Integrative Plant Biology*, *47*, 271–282.

Zhong, L., Su, Z. B., Ma, Y. M., Salama, M. S., & Sobrino, J. A. (2011). Accelerated changes of environmental conditions on the Tibetan Plateau caused by climate change. *Journal of Climate*, *24*, 6540–6550. https://doi.org/10.1175/Jcli-D-10-05000.1

Zhou, H., Zhou, L., Zhao, X., Liu, W., Li, Y., Gu, S., & Zhou, X. (2006). Stability of alpine meadow ecosystem on the Qinghai-Tibetan Plateau. *Chinese Science Bulletin*, *51*, 320–327. https://doi.org/10.1007/s11434-006-0320-4

Zhou, H. K., Yao, B. Q., Xu, W. X., Ye, X., Fu, J. J., Jin, Y. X., & Zhao, X. Q. (2014). Field evidence for earlier leaf-out dates in alpine grassland on the eastern Tibetan Plateau from 1990 to 2006. *Biology Letters*, *10*(8). https://doi.org/10.1098/rsbl.2014.0291